Audio Engineering Society

Convention Paper 10391

Presented at the 149th Convention
Online, 2020 October 27-30

Low-Frequency Performance of a Woofer-Driven Flat-Panel Loudspeaker (Part 1: Numerical System Analysis and Small Signal Measurement)

Benjamin Zenker[1], Robert Schurmann[1], Sebastian Merchel[1], and M. Ercan Altinsoy[1]

[1]*Chair of Acoustics and Haptic Engineering, Dresden University of Technology, 01062 Dresden, Germany.*

Correspondence should be addressed to Benjamin Zenker (benjamin.zenker@tu-dresden.de)

ABSTRACT

The low-frequency performance of loudspeakers is essential to the listener preference rating. To achieve the same low-frequency performance as conventional speakers, an optimized construction of a woofer-driven flat-panel loudspeaker was designed. The woofer radiates in a small air gap between the panel and the distance plate and excites the panel uniformly. At low frequencies, significant improvements compared to an exciter and a comparable performance to a conventional woofer system could be reached. This paper presents a numerical system analysis of the paneled woofer design, which provides a detailed understanding of the system's behavior. Furthermore, the radiation mechanism is compared to that of an exciter. All simulation models are comprehensively validated with the corresponding experimental data.

1 Introduction

Smart devices make it easier than at any other time to listen to music in every room. An upcoming practical problem is the simple integration of several devices in the living area. Therefore, the size of the speakers is limited, and it is becoming increasingly challenging to reproduce the audio signal with sufficient amplitude and quality[1]. As a result, flat-panel loudspeakers are becoming increasingly important for today's consumer market [2]. Those speakers make it possible to integrate large and more powerful devices in places such as the front of cabinets, which do not disturb the customer's view or disrupt the aesthetics of the room. Flat-panel loudspeakers need to reproduce a wide frequency range and high sound pressure output with acceptable signal distortion to compete with conventional speaker systems. It is well known that the low-frequency performance of loudspeakers is essential to the listener preference rating [3, 4, 5]. In a comparison of 13 different loudspeakers, Olive [4] has shown that the bass is a critical attribute underlying the preference rating of a loudspeaker. Furthermore, the low-frequency extension LFX as a -6 dB point has been used as one of four criteria to estimate the preference rating of loudspeakers[5]. Especially the low-frequency range is a physical problem for flat panel loudspeakers. At low frequencies, the modal density is low on logarithmic frequency spacing, only a few modes are excited, and the exciter's positioning becomes essential to reach a flat response [6, 7]. At high frequencies, the mode density is sufficiently high, the positioning is not important, and the response is flatter.

In order to improve the low-frequency performance of

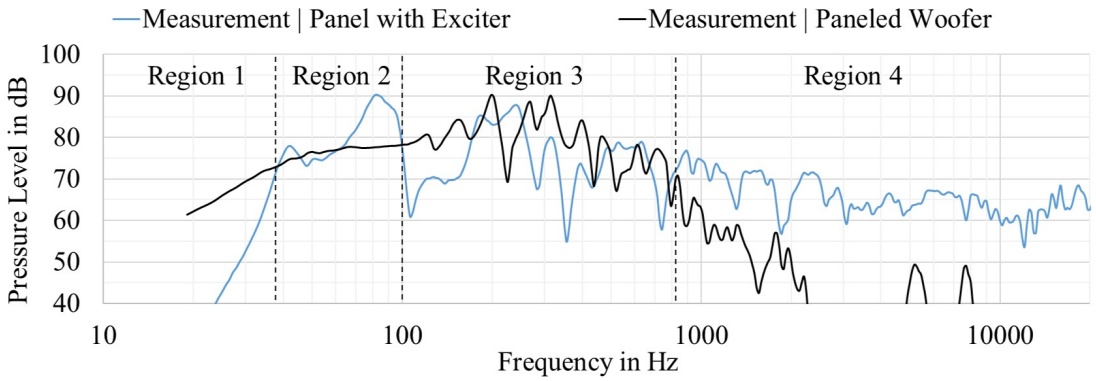

Fig. 1: Comparison of the pressure level of the panel with exciter and the paneled woofer design measured in 1 m distance with 2.83 Vrms input under free-field conditions.

flat panel loudspeakers, various constructions are already known. Anderson et al. [8] suggested using an array of force drivers to selectively excite the lowest bending mode of flat-panel loudspeakers to approximate the characteristics of conventional loudspeakers. This construction improves the behavior at low-frequencies, yet it increases the cost by the high number of drivers needed and the number of individual controlled outputs of the DSP amplifier. Another design is presented in [9], in which a conventional woofer radiates into a small air gap between the panel and a separation plate and excites the panel uniformly. The design needs no opening, and the woofer is integrated invisibly into the flat-panel loudspeaker. This design is already used in products and shows sufficient results in the low-frequency range [2]. Therefore, this design will be a central part of this paper and will be compared to a conventional woofer design and to the excitation with an exciter.

Figure 1 shows a comparison of the frequency response of a panel with an exciter and the paneled woofer design for the same panel made out of mineral material and with a movable surface of 0.3 m^2. The frequency responses can be subdivided into four different regions. In the first region, the paneled woofer generates a significantly higher SPL. Below the exciter's eigenfrequency, the magnet vibrates only without exciting the panel. In region two, the exciter driven flat-panel loudspeaker radiates effectively as the paneled woofer, caused by the directly excited modes due to the optimal exciter position. In section three, a considerably flatter transfer function can be observed. Contrary, the exciter driven panel generates a frequency response containing larger dips. In the last region, the panel with exciter presents a flatter frequency response, as the panel's modal density is high. The paneled woofer is limited, which is caused by the coupling to the air compliance. It has to be established that due to the different excitation methods, two diverse frequency responses are obtained, although the sound radiating panel is identical.

This paper focuses on the paneled woofer design, which offers a sufficient low-frequency performance combined with invisible integration. A numerical system analysis of the paneled woofer design is presented, which provides a detailed understanding of the system's behavior. Furthermore, the paneled woofer design is compared with a conventional system and a point excitation with an exciter. The present paper is intended to answer the following questions:

- How does the paneled woofer design works in detail?
- Why is the low-frequency performance improved by using a paneled woofer design compared to a panel with exciter?
- Is it possible to achieve the same low-frequency performance as a conventional system?
- Which modes are important for the radiation and how are these excited with different excitation mechanisms?
- How accurately can a multiple coupled numerical simulation model describe the system's behavior?

This paper describes the first part of a two-part analysis, in which the small-signal behavior is analyzed. The second part deals with the numerical system optimization and the large-signal analysis.

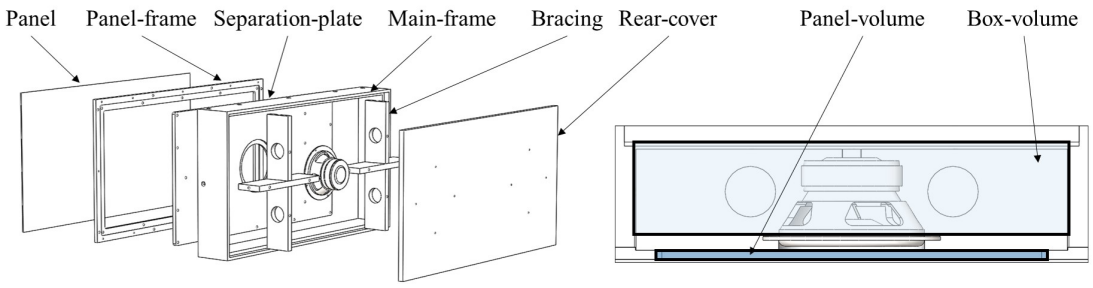

(a) Exploded view - adaptable prototype (b) Sectional view – volume definition

Fig. 2: Drawings of the adaptable prototype (a) in exploded view and (b) in sectional view to define both volumes: Box and panel volume.

2 Protoype and Reference Tests to a Conventional System

The following section introduces the adaptable prototype. This allows a direct comparison of different configurations of the flat-panel loudspeaker. Additionally, this part of the study introduces the measurement environment and presents information about the near-field effects and the applied room correction. At the end of this section, the conventional woofer design is compared with the paneled woofer design.

2.1 Adaptable Prototype

For the following analyses, an adaptable prototype was constructed in order to evaluate various configurations of the flat-panel loudspeaker under similar conditions. An exploded view of the adaptable prototype is shown in Figure 2(a). The prototype has overall dimensions of 855 mm x 467 mm and is designed for panels with an area of 0.3 m^2. The panels are glued on the 40 mm wide panel-frame to ensure rigid boundary conditions. The prototype was designed in such a way that the following features and properties can be varied:

- panel: Thickness and material properties,
- separation plate: Different types and numbers of woofers, adjustment of the panel volume,
- main frame: Adjustment the box volume and change between vented and sealed system, and

The additional bracing is very crucial to suppress vibrations of the separation plate and the rear cover, which could have a high impact on the pressure response due to the large dimensions of the prototype.

2.2 Acoustical Measurement

All acoustical measurements were performed at the anechoic chamber at the Technical University Dresden with the following equipment:

- Microphone: Gras 40HL (Low-noise),
- Power Module: Gras 12AK,
- Measurement system: Klippel DA2.

It is known that even the largest anechoic chamber is limited to lower frequencies. In this case the critical frequency f_c is 70 Hz, below f_c a correction is essential. The correction curves were estimated as shown in Figure 3. The compensation function H_c was calculated based on a reference measurement with Klippel near field scanner (NFS) and the in-situ tests at a certain location in the anechoic chamber. The resulting compensation function is applied for all measurements below f_c. The applied room-correction curve has a range of +/- 2.5 dB in the frequency range of 20 Hz to 70 Hz.

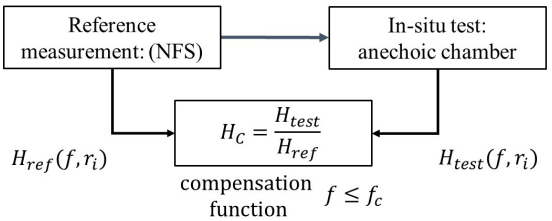

Fig. 3: Generating the compensation function based on a reference measurement with Klippel NFS and an in-situ test for low-frequency measurements in the test environment.

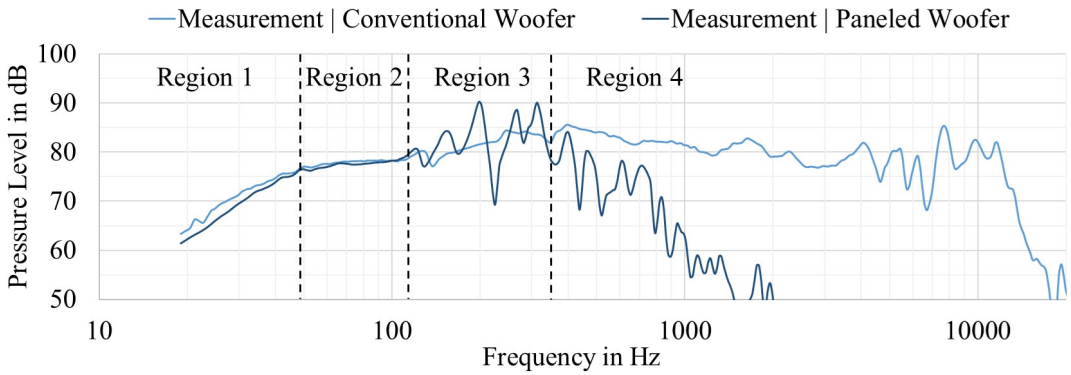

Fig. 4: Sound pressure level for 2.83 Vrms input and measured at 1 m distance on-axis of the conventional woofer design compared to the paneled woofer design under free field conditions.

2.3 Comparison of a Conventional and a Paneled Woofer System

As a first step, the evaluation of the conventional and paneled woofer design was performed. Both designs are sealed. The lower and upper cut-off frequency, the average sound pressure level, and the deviation of the transfer function were compared. For that purpose, the adaptable prototype is built in two ways, as shown in Figure 5. The first construction (a) has no panel and direct sound radiation can occur. The second construction (b) has a mineral panel with a movable area of $0.3\,\mathrm{m}^2$.

The results of the on-axis pressure response of the conventional woofer compared to the paneled woofer design are shown in Figure 4. However, both woofer designs have a comparable behavior for low frequencies, the additional panel has only a small influence according to the transfer function of the loudspeaker. This result implicates that the properties of the conventional woofer mostly influence the response of the paneled woofer. Both transfer functions have an increasing pressure level above 200 Hz, which is related to its large dimensions and an increased directivity.

For a more detailed evaluation, the graph was divided into four regions. Region 1 shows a different high-pass characteristic, which results from the additional panel stiffness below resonance frequency. Region 2 has only minor differences with less than 0.5 dB. In region 3 strong deviations occur for the paneled woofer, which is related to its modal behavior. Region 4 shows a different low-pass characteristic for both woofer designs. The upper-frequency limit of a woofer-driven flat-panel loudspeaker is much lower compared to a conventional woofer, which relates to the stiffness coupling by the panel volume and the higher moving mass of the panel with 1.84 kg compared to the lower moving mass of the cone with 0.02 kg.

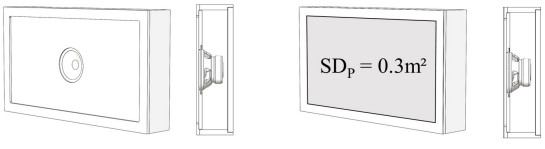

(a) Conventional Woofer (b) Paneled Woofer

Fig. 5: Comparison of the prototypes for the a) conventional woofer design and the b) the paneled woofer design.

2.4 Conclusions

The most important results of the second chapter are summarized with the following key points:

(1) An adaptable prototype is developed to evaluate various configurations with similar boundary conditions.

(2) The anechoic chamber does not satisfy the free-field conditions below 70 Hz. Consequently, a compensation function H_c was calculated by using Klippel NFS.

(3) The low frequency performance of a paneled woofer is astonishingly comparable to a conventional woofer system, which will be further analyzed in the following sections.

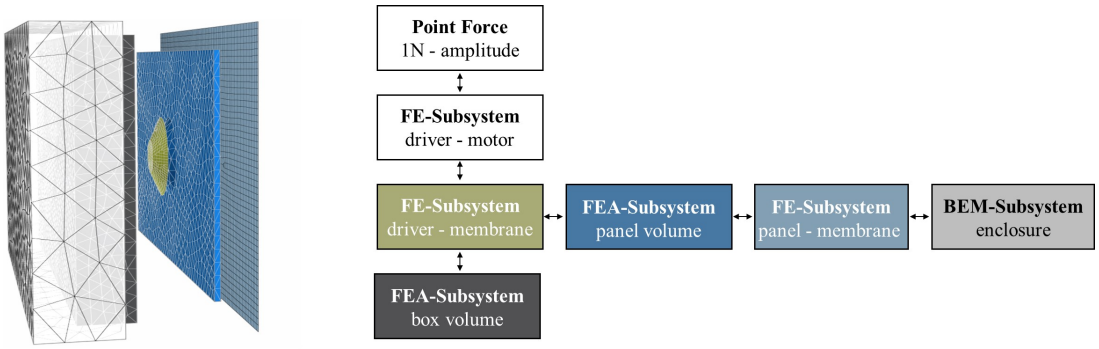

Fig. 6: Overview of the simulation model, in which (a) visualizes the individual subsystems and (b) the simulation network with the applied junctions between different subsystems of Force, FE, FEA and BEM.

3 Simulation

In the following section, the numerical simulation model of the flat panel loudspeaker is introduced and validated. The simulation model represents a more dimensional modal system, which includes FE, FEA, and BEM subsystems. This enables the coupling of the related structure and acoustical modes. The model is validated with the following steps: woofer displacement, panel displacement, and the radiated sound pressure.

3.1 Description of the Simulation Model

The simulation model was built up in the simulation software tool wave6 [10] and is based on a multiple coupling of different subsystems illustrated in Figure 6. The model consists of structural and acoustical finite element (FE)-subsystems, which are representing the driver, the panel, the box volume, and the panel volume. Furthermore, a BEM-subsystem is used to calculate the acoustic radiation. The system is woofer driven, so the driver represents the excitation, which is modeled analogously to the equivalent electro-mechanical circuit shown in Figure 7. The driver is represented by a two-part FE-subsystem consisting of the voice coil and the driver's membrane. First, the input voltage is transmitted by the electrical impedance, facing the primary and secondary resistances and inductors of the voice coil. Due to the electro-mechanical analogy, the input voltage is modeled as a point force, which is applied to the voice coil FE-subsystem. After that, a transfer matrix, including the woofer's force factor Bl is implemented. This represents the magnetic field and enables the transfer of an electrical voltage into a velocity. The mechanical part of the driver can be described by the mechanical impedance, including compliance C_{MS} and damping of the woofer's suspension R_{MS}, whereas the mass M_{MS} is applied by the FE-model of the driver's membrane. Applying the linear model of Agerkvist and Ritter [11], an exact modeling of the visco-elastic behavior of the transducer's compliance $C_{MS}(f)$ in the small signal range is possible, as demonstrated in Equation 1.

$$C_{MS}(f) = C_0 \left(1 - \kappa log_{10} \left(\frac{j\left(\frac{f}{f_{min}}\right) e^{jtan^{-1}\left(\frac{f}{f_{min}}\right)}}{\sqrt{1+\left(\frac{f}{f_{min}}\right)^2}} \right) \right) \tag{1}$$

On the rear side, the driver is connected to the box volume and on the front side to the panel volume. Both volumes are sealed and modeled by an acoustical finite element system (FEA). The stiffness of the air spring and the acoustical chamber modes can be faced at the

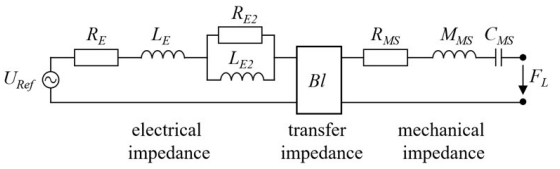

Fig. 7: Equivalent electro-mechanical circuit of a woofer.

same time. The panel volume transfers the pressure produced by the driver on the panel-membrane modeled by an FE-subsystem. The panel is clamped on the edges. The simulation of the sound radiation is provided by the coupling of the FE subsystem with the BEM subsystem. A convergence analysis with an h-refinement was performed to estimate the FEM-solution error based on the difference of the calculated eigenfrequencies. The used element length of 10 mm QQUAD8 FE-elements causes an error of less than 1 %. Based on Marburg [12], more than six elements per wavelength are used to calculate this model. The BEM subsystem is meshed with TRIA10 elements with a medium element-size of 25 mm, which has shown a convergence for this element size.

3.2 Validation of Small-Signal Behavior

As a first step, the force of the systems is validated. Therefore, the TSP and displacement of the dust cap and the magnet were measured using the Lumped-Parameter-Module (LPM) of the Klippel Analyzer 3. Because of the simultaneous measurement of the displacement via laser and the electrical parameters, respectively voltage and current, the LPM can fit the electro-mechanical model with values shown in Table 1. By comparing the TSP of the exciter and the woofer, the different constructions are noticeable. Due to the high moving mass of the exciter magnet, the magnet must be stabilized by a very stiff suspension. The suspension of the exciter is about 20 times stiffer than that of the woofer. Even if the exciter mass is higher, its natural frequency is almost twice as high. Furthermore, the exciter has a weaker magnetic field Bl and a higher resistance R_E which reduces its force compared to the woofer.
Based on these TSP the simulation was set up with the mechanical, transfer and electrical impedance. The

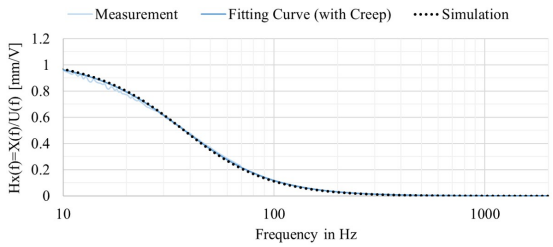

Fig. 8: Measured, fitted, and simulated transfer function Hx(f) of the driver DA175-8 in free-air.

Table 1: TSP of the woofer Dayton DA 175-8 and the Exciter Visaton EX60

Parameter	Woofer-DA175	Exciter-EX60
M_{ms} in g	20.68	115.15
R_{ms} in kg/s	2.07	4.03
K_{ms} in N/mm	0.89	17.54
Bl in N/A	6.28	5.15
f_s in Hz	32.9	62.1
R_e in Ω	5.99	6.97
L_e in mH	0.512	0.122
R_{e2} in Ω	3.46	2.11
L_{e2} in mH	0.635	0.082

mass of the driver FE-subsystem was modified to match the experimentally identified moving mass. In Figure 8, the simulated and measured displacement of the driver's dust cap is illustrated. The LPM calculates a fitted curve considering the electro-mechanical model and non-linear creep behavior of the woofer's suspension. The simulation model predicts the woofer's displacement accurately and the system's excitation is validated. The force of the woofer is nearly 40 % higher compared to the exciter, which will result in a +3 dB shift in the pressure response for the same U_{rms}. This has a minor effect on the following results. On the one hand, it will be shown that the principle of radiating a punctual force excitation is more inefficient, and on the other hand, woofer's mostly have a stronger motor due to it's larger dimensions.

3.3 Validation of the Panel Displacement

Further, the mechanical coupling between the woofer and the panel needs to be verified. Therefore, the dis-

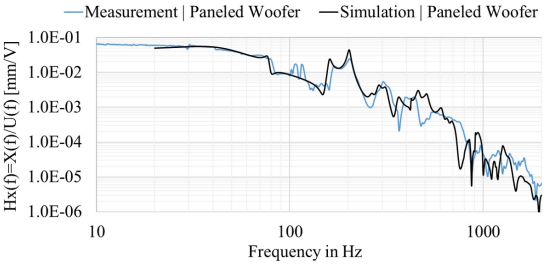

Fig. 9: Measured and simulated transfer function Hx(f) of the paneled woofer validated at the center point of the panel.

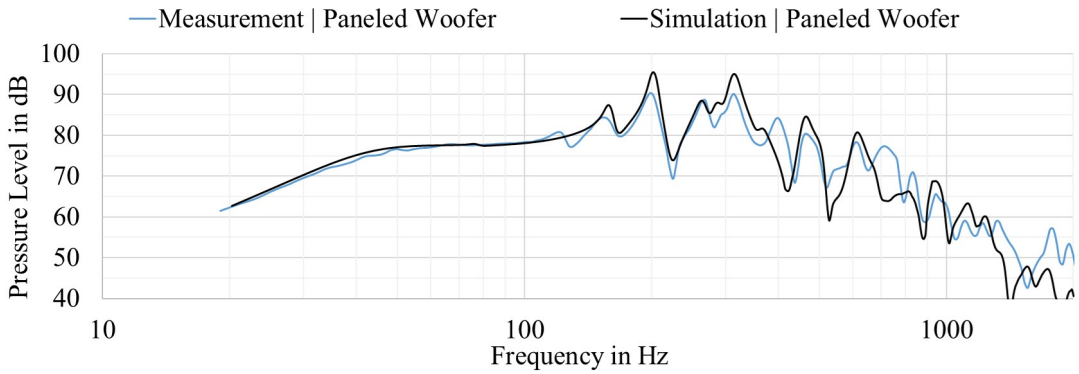

Fig. 10: Pressure level of the measured and simulated paneled woofer at 1 m distance, under free-field conditions and with 2.83 Vrms input.

placement at the center point is compared. It is sufficient to analyze a single point at the center of the panel. At lower frequencies, simpler mode shapes are existing, and the center represents the highest displacement leading to a high measurement resolution. The panel displacement was measured with the Transfer Function Measurement Module of the Klippel Analyzer 3. In combination with the Keyence HK-052 laser, a sufficient SNR up to 2 kHz was reached.
In Figure 9, the measured and simulated panel displacements are compared. Up to 400 Hz both transfer functions are very similar. However, more significant deviations appear at higher frequencies, as the influence of the acoustical volume modes rises. This deviation is not relevant for the statements of this paper, but should be analyzed in the following studies.

3.4 Validation of the Pressure Level

For low frequencies, this loudspeaker can be assumed as a point source. In consequence, the evaluation of the SPL at a single position is sufficient. The paneled woofer was measured in the anechoic chamber at a distance of 1 m on-axis. In Figure 10, the simulated and measured SPL transfer functions are shown.
It can be seen that below 100 Hz the pressure levels, are almost identical. Above 100 Hz, the system is modal driven, so the panel's eigenmodes predominantly determine the acoustical radiation. There is a slight frequency shift between the measured and simulated resonances in the amplitudes, which is related to the modal or the acoustical damping.
However, the system behavior can be described in detail. Despite the complex superposition of different subsystems, the deviation in the frequency band between measurement and simulation is small. This model can be used for the following considerations to analyze the individual radiating modes, the influence of the chamber modes, and to extract the individual radiating components with a sound-pressure related decomposition. In the second part of this paper [13] this model is used to increase the sensitivity and optimize the flatness of the response. The driver properties and the panel properties are adjusted, and general guidelines are developed.

3.5 Conclusions

The key results of the third section are summarized below:

(1) The TSP of the woofer and the exciter show their different construction and the possibility of more output by using the paneled woofer design.

(2) The woofer driven excitation can be modeled by using the electrical and mechanical impedances based on the equivalent electro-mechanical circuit.

(3) The paneled woofer is modeled as a multiple- coupled system with FE, FEA and BEM subsystems.

(4) The simulation results showing a good fit for the displacement of the paneled woofer at the center position, as well as, the radiated SPL on-axis. The simulation model is sufficiently accurate for detailed analyzes in the following sections.

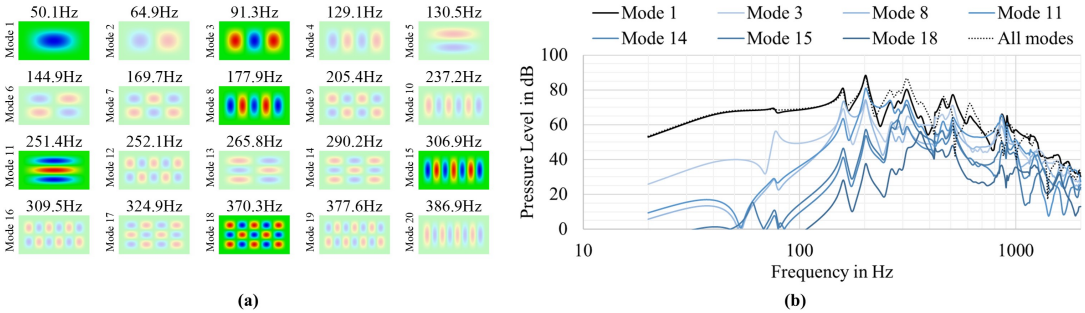

Fig. 11: Structural-modes-related decomposition. (a) Visualization of the first 20 eigenmodes of the panel with fixed boundary conditions, (b) modal contribution of all panel modes.

4 Numerical System Analysis - Paneled Woofer

In the following section, the validated simulation model is used to analyze the radiation characteristic of the paneled woofer design. The individual influence of acoustical chamber and structural eigenmodes due to the sound radiation is separated. Furthermore, the surface displacement and pressure response is decomposed in in-phase, anti-phase, and quadrature components to evaluate their frequency dependent behavior.

4.1 Structural-Modes-Related Decomposition

The structural-modes-related decomposition is necessary to identify the radiating modes of the panel. These results can be extracted directly out of the simulation software, shown in Figure 11. It can be concluded that only uneven eigenmodes are able to radiate sound by an uniform excitation. Even panel modes do not contribute to the radiation. This is caused by the destructive interference of the phase-shifted deflections on the panel surface. The resulting effective radiating panel surface is zero. In consequence, only uneven eigenmodes have an effective radiating panel surface that differs from zero.

Especially the first eigenmode is responsible for the sound radiation. Higher-order modes have a less significant impact. Mode 1 has a large radiating surface, and the panel vibrates fully in-phase. The out-of-phase vibrating areas arise upon higher eigenmodes, leading to a loss of the effective membrane surface.

Furthermore, a frequency shift is recognizable, when comparing (a) and (b) in Figure 11. The modal resonance peaks occur at frequencies, which are different from the eigenfrequencies of the panel with fixed boundary conditions. It can be assumed that the panel eigenmodes are shifted due to the additional compliance of the air cavity provided by the panel volume. A detailed description of these effects, based on an electro-mechanical model, can be found in the second part of this paper [13].

4.2 Separation of the Chamber Modes

Acoustical chamber modes can occur within the box volume and the panel volume. Both volumes have an individual influence due to the deviations in the frequency response. This influence can be separated by simulating the model with and without chamber modes of the individual subsystems. However, the first chamber mode is solved for all cases. which represents the constant pressure mode.

Figure 12 illustrates the different influence of both acoustical volumes due to the simulated pressure level on axis. The results of an ideal model without chamber modes are compared with the results of a model with only panel volume modes against a model with only box volume modes. The chamber modes of the box volume are generating small additional deviations in the frequency response. If the chamber mode of the panel volume has an extremum at the woofer's position, they affect the pressure response in a narrow band of the chamber eigenfrequency. However, the overall influence is negligible. This is not the case for the chamber modes of the panel volume. Their influence is much more significant and results in large deviations in the frequency response starting at frequencies above 350 Hz. Furthermore, only asymmetrical chamber modes contribute to the sound radiation, which is similar to the mechanical modes. By using the paneled

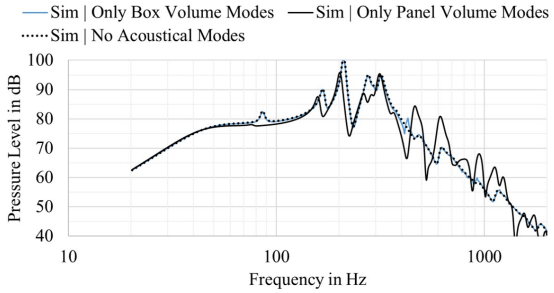

Fig. 12: Simulated pressure level to visualize the influence of the acoustical chamber modes of the individual subsystems (box volume and panel volume) compared to an ideal result without acoustical chamber modes.

woofer design, the chamber mode's influence is negligible below 350 Hz. The chamber modes will be shifted to lower frequencies by increasing the dimensions of the flat-panel loudspeaker. In most cases, the dimensions will be smaller and the influence of the chamber modes are at higher frequencies.

4.3 Sound-Pressure-Related Decomposition - Theory

The simulation model contains a considerable amount of complex vibration data, which needs to be post-processed to get the relevant information. Klippel and Schlechter [14] present efficient post-processing to separate the sound-pressure-related components of the surface vibration by using the vibration and radiation properties of a loudspeaker or a panel to decompose the radiation characteristics. Their idea is to decompose the structural vibration to identify regions on the loudspeaker or panel, which effectively contribute to the total radiated pressure level at a certain point. The separation contains the following components: in-phase, anti-phase, and quadrature components. The in-phase components have a constructive contribution to the sound radiation. In contrast, the anti-phase components counteract to the sound radiation. The quadrature components have no contribution to the radiated sound at all. They generate a similar size of vibrations with the opposite phase. The separation is implemented in relation to a reference phase ϕ_{ref} and shown in the following Equations (2) to (4).

$$\bar{x}_{in} = Re^{+}\left(\hat{x}\frac{e^{j\phi_x}}{e^{j\phi_{ref}}}\right)e^{j\phi_{ref}} \tag{2}$$

$$\bar{x}_{anti} = Re^{-}\left(\hat{x}\frac{e^{j\phi_x}}{e^{j\phi_{ref}}}\right)e^{j\phi_{ref}} \tag{3}$$

$$\bar{x}_{quad} = Im\left(\hat{x}\frac{e^{j\phi_x}}{e^{j\phi_{ref}}}\right)e^{\left(j\phi_{ref}+\frac{\pi}{2}\right)} \tag{4}$$

Another parameter that needs to be considered is the accumulated acceleration level (AAL). The total AAL represents the potential output of a system without acoustical cancellation by using the absolute values of the total mechanical vibration. The AAL is comparable with the pressure level at a observing point $\vec{r}_a$ in the far-field while neglecting any phase information. As shown in Equation 5 the total mechanical displacement $\bar{x}_{total}$ is the sum of the in-phase components $\bar{x}_{in}$, the anti-phase components $\bar{x}_{anti}$, and the quadrature components $\bar{x}_{quad}$.

$$\bar{x}_{total} = \bar{x}_{in} + \bar{x}_{anti} + \bar{x}_{quad} \tag{5}$$

By using a Rayleigh integral, shown in Equation 6, the potential amplitude of the sound pressure at the observing point $\vec{r}_a$ can be calculated. The panel displacement $\bar{x}$ is integrated over the panel surface S_p with all individual panel positions $\vec{r}_p$, to estimate the free-field radiation. Small changes in the calculation to the equations in [14] are made.

$$\bar{p}(\vec{r}_a) = \frac{\rho_0\omega^2}{4\pi}\int_{S_p}\frac{\left|\bar{x}(\vec{r}_p)\right|}{\left|\vec{r}_a-\vec{r}_p\right|}dS_p \tag{6}$$

$$AAL(\vec{r}_a) = 20log\left(\frac{\bar{p}(\vec{r}_a)}{\sqrt{2}p_0}\right)dB \tag{7}$$

In addition, the resulting sound pressure at the observing point is calculated from the pressure components of the in-phase and anti-phase components as shown in Equation 8

$$\bar{p}_{total} = \bar{p}_{in} + \bar{p}_{anti}. \tag{8}$$

Furthermore, the following relationships are valid. The in-phase component AAL_{in} can be larger than the total SPL_{total}, but never exceeds the AAL_{total}. However, a small difference between the in-phase AAL_{in} and anti-phase component AAL_{anti} causes acoustical cancellation and dips in the SPL_{total}. The quadrature component produces no sound pressure but the AAL_{quad} may exceed the in-phase component AAL_{in}.

$$AAL_{total} = AAL_{in} + AAL_{anti} + AAL_{quad} \tag{9}$$

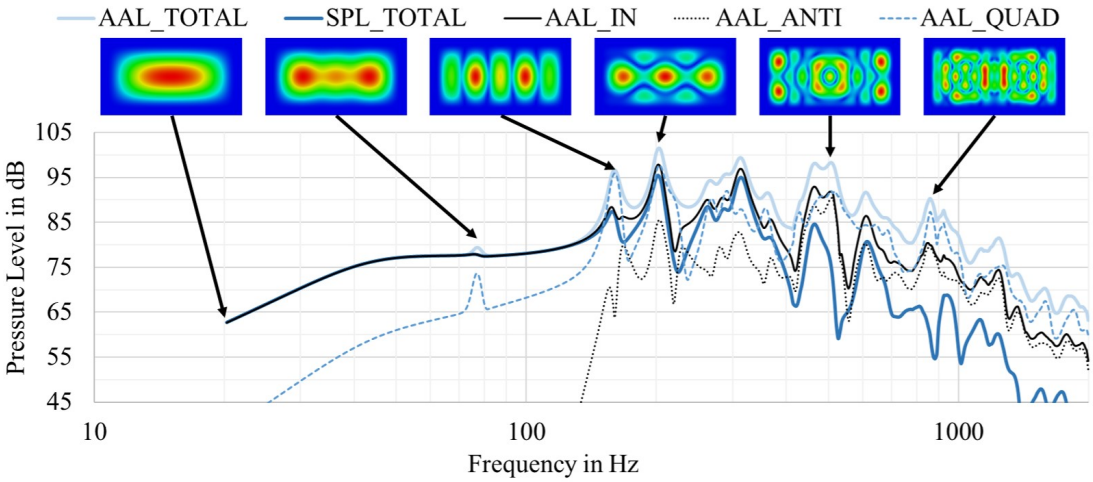

Fig. 13: Sound-pressure-related decomposition for the paneled woofer with AAL(Total), SPL(Total) AAL(In), AAL(Anti), and AAL(Quad).

4.4 Sound-Pressure-Related Decomposition for the Paneled Woofer

The results of the sound-pressure-related decomposition are shown in Figure 13. It is evident that the panel has only in-phase components up to 150 Hz, which indicates a very efficient radiation. There are no anti-phase components and a minimum of quadrature components. The anti-phase and quadrature components are increasing with rising frequency, in which the anti-phase component is significantly lower than the in-phase component up to 300 Hz. Below the eigenfrequency of the first mode, the anti-phase component is low. After the peak of the first eigenmode the anti-phase component has a similar level as the in-phase component. At this point, the radiation becomes much more inefficient. Furthermore, an indirect upper-frequency limit can be seen due to the compression of the air volume by the decrease of the AAL to higher frequencies. The high-frequency characteristic is determined by the compression of the air volume, the high moving mass of the panel, and the reduced usable radiating surface. However, the usable frequency range of this construction is up to 300 Hz. This allows an improved low-frequency radiation, but it is necessary to use an additional exciter for higher frequencies.

4.5 Conclusions

(1) The sound radiation is driven by uneven panel modes. Modes of even order have no effective radiating surface by exciting them with a homogeneous surface load.

(2) The radition efficiency of a structural panel mode depends on the effective radiating surface. This is the largest for the first eigenmode, and reduces for more complex modeshapes.

(3) Acoustical chamber modes occur within the box volume and the panel volume. They predominantly affect the deviations at higher frequencies. For lower frequencies their influence is negligible.

(4) The sound pressure can be decomposed in in-phase, anti-phase and quadrature components, by considering the complex vibration data and the radiation properties. This enable a calculation of the maximum potential output of a loudspeaker by using the AAL, which neglects the phase information.

(5) The paneled woofer is an efficient design with only in-phase components at lower frequencies. However, the usable frequency range is limited to higher frequencies. Therefore, it is necessary to use an additional exciter for higher frequencies.

(6) The sound-pressure-related decomposition is a useful tool to compare different radiation mechanisms and allows a much deeper understanding compared to the pressure response.

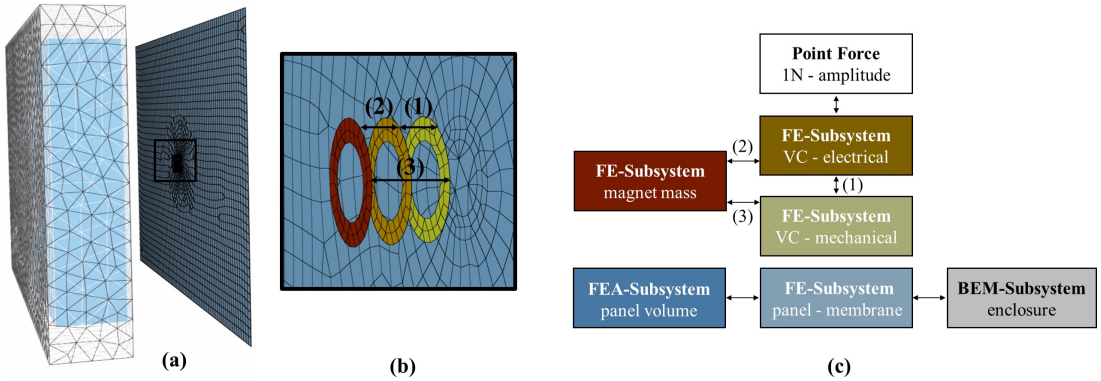

Fig. 14: Overview of the simulation model, in which (a) visualizes the individual subsystems and (b) the simulation network with the applied junctions between different subsystems of Force, FE, FEA and BEM.

5 Numerical System Analysis - Panel with Exciter

In the following section, the homogeneous panel excitation of the paneled woofer design is compared with a local force excitation of an exciter. The exciter is placed at the center position, which enables the highest sensitivity for lower frequencies, but will result in higher deviations in the frequency response. The exciter differs from conventional woofer. The magnet has a separate degree of freedom (DOF) and is able to move independently to the front. This results in a different low-frequency behavior. Furthermore, the exciter is placed at a certain position on the panel. Therefore, the displacement occurs mostly at that point but can differ over the whole surface. For these reasons, the characteristics are expected to be very different. In the first part both DOF are measured and their individual movements are analyzed. Further, the measurement data is validated with the simulation model, which will be used to analyze the mode related radiation characteristics of the exciter driven panel. These results are compared to the behavior of the paneled woofer design.

5.1 Two Degrees of Freedom - Displacement of the Panel and the Exciter Magnet

A sufficient low-frequency validation, between experimental and numerical analysis is the evaluation of the surface displacement at two points of the vibration system. Point one is at the center of the panel and the other one is the movement on the magnet. Both cases are measured with the TRF module of Klippel KA3 and evaluated as the transfer function Hx(f) shown in Figure 15. It is important to differentiate both individual movements. Region 1 describes the behavior below the resonance frequency of the exciter and below the first-panel mode. The panel is below the resonance frequency stiffer than the exciter's suspension. This results in a low displacement of the panel and a high displacement of the exciter. Practically, nearly no force of the exciter will be transferred to the panel. Instead, it is only converted into the movement of the magnet. Therefore, the fundamental of the pressure level is small, and high harmonic distortion will be produced. This will limit the maximum SPL. Additionally, the mass of the exciter lowers the eigenfrequency of the panel and the whole system. In region 2, an interaction of the individual panel modes and the exciter

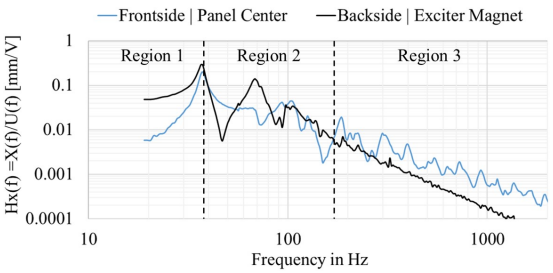

Fig. 15: Measured transfer function Hx(f) of the front side of the panel with exciter and the backside of the magnet to visualize their individual frequency dependent behavior. The chosen panel is open and no additional stiffness of the air volume is applied.

mode occurs, which results in similar displacement levels. Furthermore, the exciter magnet displacement is strongly frequency-dependent with peaks and dips in the displacement. Above 150 Hz (region 3), the exciter magnet movement is reduced and decreases more rapidly than the displacement of the panel. The influence of the exciter's resonance is no longer given, and both systems are moving independently. The system's resulting total force is divided into the force of the panel movement and the force of the magnet movement. This effect can be pretended by fixing the magnetic mass, as mentioned by Klippel [15]. This will result in a less steep high-pass filter. Due to the lower mass of the whole system (as a result of the fixed magnet), the eigenfrequency will increase, but the distortions will decrease significantly.

5.2 Simulation Model of the Exciter Driven Panel

The simulation model of the exciter driven panel is different from the simulation model of the paneled woofer. As shown in Figure 14, the exciter itself has two degrees of freedom (DOF): The voice coil and the moving mass of the magnet. The stiffness of the spider couples both subsystems. As mentioned in [16] the resonance frequency of the magnet is much more critical compared to the resonance frequency of the voice coil. Therefore, both DOF must be modeled for the system with a complete numerical system analysis. The force of an exciter is represented by three subsystems. The electrical subsystem represents the electrical part of the electro-mechanical network. Furthermore, the mechanical part of the voice coil has to be simulated with the mass of the voice coil. Additionally, the high mass of the magnet needs to be modeled as a separate subsystem. This subdivision allows the coupling of the individual subsystems via transfer matrices. In the electrical domain, the magnet and the voice coil are coupled to the electrical subsystem via the transfer matrix of the magnetic field *Bl*. Moreover, there is also a coupling of the magnet with the mechanical subsystem of the voice coil via the spider. This allows an individual movement of both DOF of the exciter.

5.3 Validation of the Panel and the Exciter Displacement

In the case of the exciter, it is important to validate both degrees of freedom. Therefore, the validation of the displacement takes place with an open backside

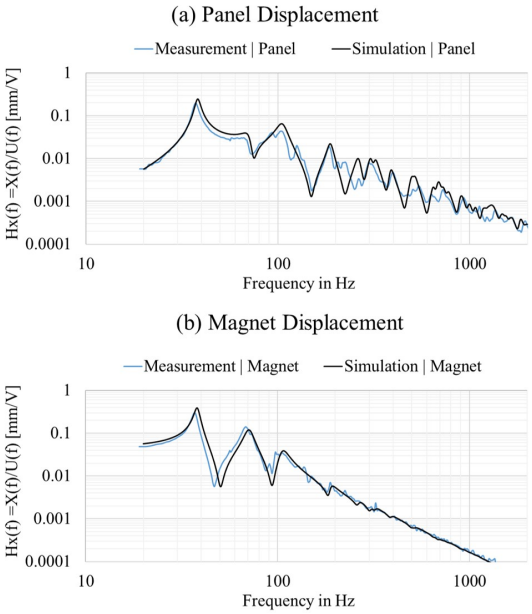

Fig. 16: Measured and simulated transfer function Hx(f) (a) of the frontside of the panel with exciter and (b) the backside of the magnet. The construction has an open backside and no additional stiffness of the air volume is applied.

to measure the displacement on the panel and the exciter under same conditions. The additional stiffening due to the enclosed air volume will shift the first-panel mode to higher frequencies, but will not change the transfer functions of the panel and exciter substantially. The panel displacement was measured with the TRF module and the Klippel KA3 in combination with the low-noise laser Keyence HK-052, which is enabling a sufficient SNR up to 2 kHz.
However, Figure 16 shows the frequency-dependent panel displacement at the center position and the magnet displacement, validated with the simulation results. It is noticeable that the displacements are accurately described by the model at lower frequencies. For higher frequencies, the displacements on the panel at the center position are slightly higher in the simulation model than in the measurement. Therefore, it is necessary to validate the entire surface in a second step to identify the source of this difference in detail. For the following conclusions, this model fit is sufficient to calculate the sound-pressure related decomposition with high accuracy.

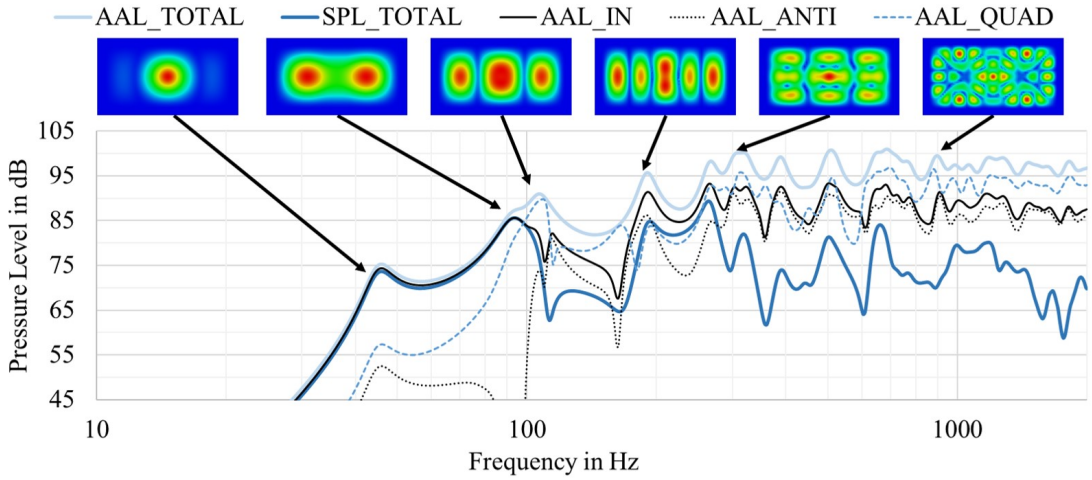

Fig. 17: Sound-pressure-related decomposition for the panel with exciter: AAL(Total), SPL(Total) AAL(In), AAL(Anti), and AAL(Quad).

5.4 Validation of the Pressure Level

As an addition to the mechanical system behavior, the acoustical properties need to be validated. The panel with exciter force was measured in the anechoic chamber at a distance of 1 m on-axis and with 2.83 Vrms input. In Figure 18 the simulated and measured SPL transfer functions are shown. As mentioned in the previous subsection, a small shift occurs between the simulation model and the real measurement. This shift is acceptable since the shape of the curve fits the measurement, single modes are individual shifted, and both vibration systems are working correctly. However, the steep decay at low frequencies can be described accurately. Furthermore, an increase at 90 Hz, and a deep dip of about 25 dB in the range of 110 Hz - 150 Hz are clearly displayed in the simulation model. Additionally, the pressure level increases again by 20 dB at 180 Hz, and the following individual peaks and dips are showing only a minimal frequency shift between the simulation model and the measurement. However, the acoustic measurement of the pressure level has a substantial disadvantage. It does not give any information about the causes of the large deviations in the pressure level response. Do they occur because of a missing force in the panel and a wide gap between the modes, or do the modes generate strong anti-phase components that minimize the pressure level? This question will be discussed in the following subchapter.

5.5 Sound-Pressure-Related Decomposition

A complete understanding of the radiation mechanism is only possible by considering the surface displacement and the related sound pressure. Due to the high deviations of the frequency response on-axis, the causes of these deviations can be analyzed in detail by using the sound-pressure-related decomposition.
Figure 17 visualizes the sound pressure-related decomposition for the panel with exciter. The result differs significantly from the results of the paneled woofer. At low frequencies, the local excitation on the panel produces anti-phase components in addition to the in-phase components. These are visible in the surface displacement at 40 Hz. This anti-phase component results from an additional bending of the panel. The force

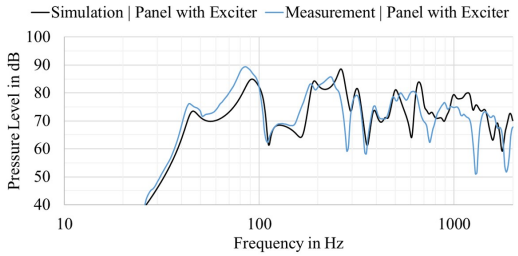

Fig. 18: Validation of the measured and simulated pressure response of the panel with exciter in 1 m distance and with 2.83 Vrms input.

moves the panel in-phase in center direction. Through the compression and expansion of the stiff air volume, off-center parts of the soft panel are moving in the opposite direction. This results in approx. 1 dB less output. Furthermore, the anti-phase and quadrature components are much higher at lower frequencies compared to the paneled woofer construction. At 100 Hz, the quadrature components are higher compared to the in-phase components, which happens with the paneled woofer construction at higher frequencies at approx. 150 Hz. The dip between 100 Hz, and 180 Hz does not result from an insufficient panel movement. Instead, it is caused by a large amount of anti-phase components. This cancellation can be significantly reduced by changing the position of the exciter or a change of the mode distribution [6, 7]. Further, it can be seen that the AAL does not decrease to higher frequencies. This is due to the direct coupling of the exciter to the panel. In the case of the paneled woofer, the force is applied via the panel volume indirectly. This limits the output at higher frequencies. The exciter is able to excite the panel up to the highest frequencies.

5.6 Conclusions

(1) Below the first exciter's eigenmode, the exciter's magnet has high amplitudes and the vibration of the panel is negligible low. This results in almost no sound radiation.

(2) Both DOF of the exciter can be modeled with the corresponding impedances. The displacement of the exciter's magnet and the panel are validated by corresponding experimental data and show a sufficient fit.

(3) Between the measured and simulated SPL is a small pressure shift however, the qualitative course coincides.

(4) At low frequencies, the exciter driven flat-panel speaker produces significantly more anti-phase and quadrature components than the woofer-driven system, leading to a minor acoustical performance.

(5) Large and broadband dips can be caused due to an increased portion of anti-phase components.

6 Summary

This paper introduces the paneled woofer design. This design is an alternative approach to achieve a better low-frequency performance compared to an exciter driven flat-panel loudspeaker. Furthermore, a similar low-frequency performance as a conventional driver can be achieved.
In several sections the woofer-driven flat-panel loudspeaker is compared to a conventional woofer and to a local force using an exciter. It could be shown that the paneled woofer design is mainly connected to several advantages concerning the radiation of lower frequencies leading to improved sensitivity, a lower cut-off frequency, and a flatter frequency response. However, the radiation of higher frequencies is limited.
Furthermore, a simulation model considering a woofer and exciter driven excitation is set up in the simulation software wave6. Both systems, paneled woofer and exciter, are modeled representing the electro-mechanical equivalent circuit. However, the system's behavior can be described with sufficient accuracy. The simulation is used to analyze the individual radiating modes and the influence of the chamber modes, and to perform a sound-pressure related decomposition. The key conclusions are summarized below.

(1) The paneled woofer design behaves nearly similar to the conventional woofer design in the lower frequency range.

(2) The low-frequency performance of an exciter is worse compared to the paneled woofer. Furthermore, anti-phase and quadrature components already occur at lowest frequencies.

(3) The paneled woofer design allows the usage of more powerful drivers (in the current state), compared to available exciters. Therefore, higher sensitivity and lower cut-off frequency are possible.

(4) The paneled woofer design drives unsymmetrically modes only. All symmetrical modes are suppressed, which is caused by their non radiating surface.

(5) It turns out the first eigenmode is predominantly responsible for the sound radiation. Mode 1 vibrates fully in-phase, whereas, upon the higher eigenmodes, anti-phase-vibrating areas occur, which are reducing the effective membrane surface.

(6) A simulation tool allows a detailed analysis of the radiation mechanisms and a further understanding of the frequency-dependent behavior.

(7) The sound-pressure-related decomposition is a useful tool to compare different radiation mechanisms and allows a much deeper understanding compared to the pressure response.

The paneled woofer design will be analyzed further in the second part of this paper [13]. The second part focuses on the large-signal performance of the paneled woofer design and the optimization of the frequency response by changing the driver's and panel properties.

References

[1] Klippel, W., "Green Speaker Design (Part 1: Optimal Use of System Resources)," in *Audio Engineering Society Convention 146*, 2019.

[2] Zenker, B., Merchel, S., and Altinsoy, M. E., "Rethinking Flat Panel Loudspeakers—An Objective Acoustic Comparison of Different Speaker Categories," in *Audio Engineering Society Convention 147*, 2019.

[3] Klippel, W., "Assessing the Subjectively Perceived Loudspeaker Quality on the Basis of Objective Parameters," in *Audio Engineering Society Convention 88*, 1990.

[4] Olive, S. E., "A Multiple Regression Model for Predicting Loudspeaker Preference Using Objective Measurements: Part I - Listening Test Results," in *Audio Engineering Society Convention 116*, 2004.

[5] Olive, S. E., "A Multiple Regression Model for Predicting Loudspeaker Preference Using Objective Measurements: Part II - Development of the Model," in *Audio Engineering Society Convention 117*, 2004.

[6] Zenker, B., Rawoof, S. S. A., Merchel, S., and Altinsoy, M. E., "Low Deviation and High Sensitivity—Optimized Exciter Positioning for Flat Panel Loudspeakers by Considering Averaged Sound Pressure Equalization," in *Audio Engineering Society Convention 147*, 2019.

[7] Zenker, B., Rawoof, S. S. A., Merchel, S., and Altinsoy, E., "Optimized Exciter Positioning Based on Acoustic Power of a Flat Panel Loudspeaker," in *Audio Engineering Society Convention 146*, 2019.

[8] Anderson, D., Heilemann, M., and Bocko, M. F., "Impulse and Radiation Field Measurements for Single Exciter versus Exciter Array Flat-Panel Loudspeakers." in *Audio Engineering Society Convention 143*, 2017.

[9] Hommel, M., "Lautsprecher," in *DE102015205658B4*, German Patent and Trade Mark Office - DPMA, 2015.

[10] wave6, "Software version 2020.4.4," Dassault Systemes SIMULIA Corporation, available at www.wavesix.com.

[11] Agerkvist, F. T. and Ritter, T., "Modeling Viscoelasticity of Loudspeaker Suspensions Using Retardation Spectra," in *Audio Engineering Society Convention 129*, 2010.

[12] Marburg, S., "Six boundary elements per wavelength: Is that enough?" *Journal of Computational Acoustics*, 10(1), pp. 25–51, 2002.

[13] Zenker, B., Heinl, M., Merchel, S., and Altinsoy, M. E., "Low Frequency Performance of a Woofer-Driven Flat Panel Loudspeaker (Part 2: Numerical System Optimization and Large Signal Analysis)," in *Audio Engineering Society Convention 149*, 2020.

[14] Klippel, W. and Schlechter, J., "Measurement and Visualization of Loudspeaker Cone Vibration," in *Audio Engineering Society Convention 121*, 2006.

[15] Klippel, W., "Green Speaker Design (Part 2: Optimal Use of Transducer Resources)," in *Audio Engineering Society Convention 146*, 2019.

[16] Zenker, B., Merchel, S., and Altinsoy, M. E., "Upper Frequency Limit of Flat Panel Loudspeakers - Evaluation of the Voice Coil Break-Up Modes," in *Audio Engineering Society Convention 148*, 2020.